

# The Voltage-Current Characteristic of high $T_c$ DC SQUID : theory, simulation, experiment

Ya. S. Greenberg, I. L. Novikov

Novosibirsk State Technical University, 20 K. Marx Ave., 630092 Novosibirsk, Russia

(Dated: April 14, 2024)

The analytical theory for the voltage-current characteristics of the large inductance ( $L > 100\text{pH}$ ) high- $T_c$  DC SQUID that has been developed previously is consistently compared with the computer simulations and the experiment. The theoretical voltage modulation for symmetric junctions is shown to be in a good agreement with the results of known computer simulations. It is shown that the asymmetry of the junctions results in the increase of the voltage modulation if the critical current is in excess of some threshold value (about  $8\text{ A}$ ). Below this value the asymmetry leads to the reduction of the voltage modulation as compared to the symmetric case. The comparison with the experiment shows that the asymmetry can explain a large portion of experimental values of the voltage modulation which lie above the theoretical curve for symmetric DC SQUID. It also explains experimental points which lie below the curve at small critical currents. However, a significant portion of these values which lie below the curve cannot be explained by the junction asymmetry.

PACS numbers:

## I. INTRODUCTION

The new type of superconductors, which has been discovered in the end of the last century by Bednorz and Müller, is widely used in the modern SQUID systems. The majority of high  $T_c$  DC SQUIDs are based on the YBCO thin films and have the different types of design<sup>2,3</sup>. However, the adequate theory of the voltage-current characteristic (VCC) of the high- $T_c$  DC SQUID, which would predict its transfer function and energy resolution, still not exists. In recent time intensive computer simulations and theoretical studies have been performed to investigate the dependence of high- $T_c$  DC SQUID behavior on various factors<sup>4,5,6</sup>, but a marked disagreement of the numerical simulations with experiment is still observed: the experimental transfer functions in many cases are much lower than the values predicted by theory and computer simulations; the white noise is about ten times higher than predicted. This is one of the most important unsolved problems, which seriously hinders the optimization of high  $T_c$  DC SQUIDs for applications.

Up to now the high- $T_c$  DC SQUIDs have the significant parameter dispersion, but the reasons of such dispersion are not established. One of the possible reasons for the dispersion could be attributed to the junction asymmetry of SQUID interferometer (unequal critical currents or (and) normal resistances), which for grain boundary junctions is about 20-30 percents due to on chip technological heterogeneity.

Recently, the theory of the voltage-current characteristic of the high  $T_c$  DC SQUID, which expands the validity range of the Chesca's analytic theory<sup>5</sup> on the DC SQUIDs with large inductance  $L > 100\text{ pH}$  and accounts both for the symmetric and asymmetric DC SQUIDs, was developed<sup>7,8</sup>. The theory is based on the perturbation solution of the two-dimensional Fokker-Planck equation (2D FPE) that describes the stochastic dynamics of DC SQUID in presence of the large thermal fluctuations.

In the paper the results of the analytic theory of VCC of high  $T_c$  DC SQUID<sup>7,8</sup> are compared with the computer simulations and with the experiment. It is shown that the theoretical voltage modulation for symmetric junctions is in a good agreement with the results of known computer simulations. It is also shown that the asymmetry of the junctions results in the increase of the voltage modulation if the critical current is in excess of some threshold value (about  $8\text{ A}$ ). Below this value the asymmetry leads to the reduction of the voltage modulation as compared to the symmetric case. The comparison with the experiment shows that the asymmetry can explain a large portion of experimental values of the voltage modulation which lie above the theoretical curve for symmetric DC SQUID. It also explains experimental points which lie below the curve at small bias currents (less about than  $10\text{ A}$ ). However, a significant portion of these values which lie below the curve at larger bias currents cannot be explained by the junction asymmetry.

The paper is organized as follows. In the section II we present in a concise form the main theoretical results for symmetric and asymmetric DC SQUIDs. In Section III we compare theoretical voltage-current characteristics for symmetric DC SQUID with the computer simulations of stochastic dynamical equations of DC SQUIDs which have been made earlier by other authors. In this section we also study in detail the influence of the junction asymmetry on the voltage modulation as compared with symmetric case. In Section IV we compare the theory with experiment and show that the junction asymmetry can explain a large portion of experimental points which lie well above the theoretical voltage modulation curve for symmetric DC SQUID.



## II. THE MAIN RESULTS OF THE ANALYTIC THEORY OF VCC OF HIGH $T_C$ DC SQUID

### A. Symmetric DC SQUID

We consider a symmetric DC SQUID with equal critical currents of junctions,  $I_{C1} = I_{C2} = I_C$ , equal normal resistance,  $R_1 = R_2 = R$ , and loop inductance  $L$ . The equations, describing such SQUID, have the following form:

$$\frac{L}{2R} \frac{d}{dt} \phi = \chi - L I_C \cos \phi \sin \phi' + \frac{L}{2} I_N(t) \quad (1)$$

$$\frac{\phi_0}{R} \frac{d}{dt} \phi = I - 2I_C \sin \phi \cos \phi' - I_N(t) \quad (2)$$

where  $\phi_0 = h/2e$  is a quantum of magnetic flux,  $\phi$  is a magnetic flux trapped in the interferometer loop,  $\chi$  is external magnetic flux,  $I$  is a bias current,  $\phi' = \phi - \chi/\phi_0$ ,  $\phi = \phi_0$ . The quantities  $I_N(t)$  are independent stochastic variables related to the Nyquist current noise of junctions:

$$I_N(t) I_N(t^0) = \frac{4k_B T}{R} \delta(t - t^0) \quad (3)$$

where  $k$  is the Boltzmann constant,  $T$  is the absolute temperature.

The output voltage across SQUID is the low frequency part of the equation (2), which is averaged over the noise:

$$V = \frac{\phi_0}{2} \frac{d}{dt} \phi \quad (4)$$

Thus, the stochastic equations (1), (2) are described DC SQUID behavior in presence of the thermal fluctuations. The solution of these equations depends on the following parameters: screening parameter  $\lambda = 2L I_C = \phi_0$ , noise parameter  $\eta = 2 k_B T = \phi_0 I_C$  and dimensionless inductance  $\beta = L/L_F$ , where  $L_F = (\phi_0/2)^2/k_B T$  is a fluctuation inductance, equaled 100 pH at  $T = 77$  K. But only two of them are independent due to relation  $\lambda = \beta \eta$ .

The known theoretical approaches to the solution of equations (1), (2) are based on the analysis of the equivalent two dimensional Fokker-Planck equation for the distribution function  $P(\phi; \phi')$ :

$$\frac{1}{2R} \frac{\partial P}{\partial t} = \frac{\partial}{\partial \phi} \left( \frac{\partial W}{\partial \phi} P \right) + \frac{\partial}{\partial \phi'} \left( \frac{\partial W}{\partial \phi'} P \right) + k_B T \frac{\partial^2 P}{\partial \phi^2} + k_B T \frac{\partial^2 P}{\partial \phi'^2} \quad (5)$$

where  $W$  is a two dimensional potential energy for DC SQUID:

$$W = E_J [1 - \cos \phi' \cos \phi] - \frac{i}{2} \phi + \frac{(\phi' - \phi_x)^2}{2} \quad (6)$$

$E_J = \phi_0 I_C/2$  is a Josephson coupling energy of two junctions in parallel,  $i = I/I_C$ ,  $\phi_x = \chi/\phi_0$  is a dimensionless external magnetic flux.

At the present time there exist some analytical solutions of equation (5), which are valid at different ranges of  $\beta$ ;  $\eta$ .

1) The exact analytical solution of FPE can be obtained in the small inductance limit ( $\beta \rightarrow 0$ ;  $\eta \ll 1$ ;  $\lambda \ll 1$ ). In this case SQUID is equivalent to a single Josephson junction with normal resistance  $R=2$  and critical current  $2I_C \cos \phi_x$ . The voltage across such single junction is well known and can be obtained from Ambegaokar-Halperin form<sup>9</sup>:

$$\frac{V}{R I_C} = \frac{1}{p(i; i'_x)} \quad (7)$$

where

$$p(i; i'_x) = \frac{2}{4} \int_0^{2\pi} e^{W(y)} dy \int_0^{2\pi} e^{W(x)} dx \int_0^1 e^{\frac{2-i}{2} y} \int_0^{2\pi} e^{W(x)} dx \int_0^{2\pi} e^{W(x)} dx^5 \quad (8)$$



$$W(x) = (i\omega) x + (2\omega) \cos' x \cos x \quad (9)$$

2) The approximate analytical solution of FPE (5) was obtained in<sup>5</sup>. This solution is valid at  $\omega < 0.3$  and relatively high thermal fluctuations level ( $\omega > 1$ ).

3) The original method for the solution of equation (5) for SQUID with large inductance ( $L \gg 1$ ) was presented in<sup>7</sup>. The method is based on the perturbation expansion of the solution of 2D FPE (5) over small parameter  $\epsilon = \exp(-2)$ . The result is the following expressions for voltage  $V$  across a SQUID and voltage modulation  $V = V(x = -2) - V(x = 0)$ :

$$\frac{V}{R I_C} = \frac{2}{p(i; 2; 0)} - \frac{1}{2} \exp(-2) \cos(2' x) f(i; \epsilon) \quad (10)$$

$$\frac{V}{R I_C} = \exp(-2) f(i; \epsilon) \quad (11)$$

where the value  $p(i; 2; 0)$  was defined in (8).

According to<sup>8</sup>

$$f(i; \epsilon) = \frac{256 \epsilon^3 i^2 \epsilon^3}{[p(i; 2; 0)]^2} B^2 \quad (12)$$

where

$$B = \sum_{n=1}^{\infty} \frac{(-1)^n I_n \frac{1}{i^2 + 4n^2} I_{n+1} \frac{1}{i^2 + 4n^2}}{i^2 + 4n^2} \quad (13)$$

$I_n$  is a modified Bessel function.

These expressions are valid for  $L \gg 1$  and any values of  $\epsilon$ , and  $\omega$  which are consistent with the condition  $\omega = \epsilon$ . Therefore, they can be applied for the analysis of a majority of practical high  $T_C$  DC SQUIDS with  $0.05 \leq L \leq 1$ ,  $\epsilon \leq 1$ . However, it should be remembered that Eqs.(4) and (11) are the approximate expressions which account for the first order term in the perturbation expansion of the voltage over small parameter  $\epsilon = \exp(-2)$ .

#### B. Asymmetric DC SQUID

We describe the junction asymmetry in terms of the asymmetry parameters  $R_1$  and  $R_2$ , which are defined according to:  $I_{C1} = (1 + \epsilon) I_C$ ,  $I_{C2} = (1 - \epsilon) I_C$ ,  $R_1 = R/(1 + \epsilon)$ ,  $R_2 = R/(1 - \epsilon)$ , where

$$I_C = \frac{I_{C1} + I_{C2}}{2}; \quad \epsilon = \frac{I_{C1} - I_{C2}}{I_{C1} + I_{C2}} \quad (14)$$

$$R = \frac{2R_1 R_2}{R_1 + R_2}; \quad \epsilon = \frac{R_2 - R_1}{R_1 + R_2} > 0 \quad (15)$$

The perturbation method, developed in<sup>7</sup>, has been applied to obtain the expressions for the voltage and its modulation across an asymmetric SQUID with large inductance<sup>8</sup>. Corresponding expressions have the following forms:

$$\frac{V}{R I_C} = \frac{V_0}{R I_C} - 8 \epsilon^3 e^{-2} \frac{i^4}{p_- p_+} f_S \cos(2' x + t_0) + Q \sin(2' x + t_0) g \quad (16)$$

$$\frac{V}{R I_C} = 16 \epsilon^3 e^{-2} \frac{i^4}{p_- p_+} \frac{p}{S^2 + Q^2} \quad (17)$$

where  $t_0 = (i = 2)$ ;

$$V_0 = R I_C \left[ \frac{1}{(1 - \epsilon)p} + \frac{1}{(1 + \epsilon)p_+} \right] \quad (18)$$



$$p = \int_0^Z e^{-W(y)} dy - \int_0^Z e^{-W(x)} dx - 1 - e^{-\frac{i(1-\gamma)}{2}} - \int_0^Z e^{-W(x)} dx - \int_0^Z e^{-W(x)} dx \quad (19)$$

$$W(x) = \frac{i}{2} (1 - \gamma)x + \frac{1}{2} \cos x \quad (20)$$

The quantities  $S$  and  $Q$  have the form s:

$$S = \frac{i}{2} \left( \frac{1}{p_+} + \frac{1+\gamma}{p} \right) B(\gamma; \gamma) B(\gamma; \gamma) \quad (21)$$

$$Q = \frac{B(\gamma; \gamma) A(\gamma; \gamma)}{p_+} - \frac{B(\gamma; \gamma) A(\gamma; \gamma)}{p} \quad (22)$$

where

$$A(\gamma; \gamma) = \sum_{n=1}^{\infty} \frac{(1-\gamma)^n n I_n \frac{1+\gamma}{2} I_{n+1} \frac{1+\gamma}{2}}{\frac{i}{2} (1+\gamma)^2 + n^2} \quad (23)$$

$$B(\gamma; \gamma) = \sum_{n=1}^{\infty} \frac{(1-\gamma)^n I_n \frac{1+\gamma}{2} I_{n+1} \frac{1+\gamma}{2}}{\frac{i}{2} (1+\gamma)^2 + n^2} \quad (24)$$

For  $\gamma = 1$  the expressions (16)–(24) are valid at any values of asymmetry parameters  $\gamma$  and  $\gamma$  and at any values of  $\gamma$  and  $\gamma$ , which are consistent with the condition  $\gamma = 1$ .

### III. VOLTAGE-CURRENT CHARACTERISTICS

#### A. Symmetric DC SQUID

According to (10), the influence of SQUID inductance on VCC appeared as the reduction of the apparent value of the critical current (Fig. 1). Such behavior is due to the suppression and masking of the critical current by the significant thermal current fluctuations in the interferometer loop. The more the inductance the more the suppression of the critical current. If  $\gamma \gg 1$  the second term on the righthand side of the expression (10) may be neglected and from comparison of (10) with (4) we see that in this limit the DC SQUID is equivalent to a single Josephson junction whose critical current is twice as less as that for the case  $L = 0$ .

There are two DC SQUID parameters which are easily measured: the bias current,  $I$ , and the voltage modulation,  $V$ . By the tuning of the bias current the value  $I = I_{MAX}$ , which corresponds to the maximum of the voltage modulation  $V_{MAX}$ , can be found. On the practice this guarantees the maximum of the SQUID transfer function  $dV/dI$ .

As is seen from (11) its righthand side is the product of two terms, one of them  $\exp(-2)$  depends on the SQUID inductance only, the other one depends on the bias  $I$  and critical  $I_c$  currents. The first factor describes the suppression of the critical current by the noise current in the interferometer loop. This is similar to the suppression effect in the interferometer loop with a single Josephson junction<sup>15</sup>. The second factor describes the critical current suppression by the thermal fluctuations, which is similar to the suppression effect in a single Josephson junction. The factorization allows us to carry the first factor to the left hand side of expression (11), so that we consider below the reduced modulation  $V_R = \exp(-2) V = R$ , which depends on the critical and bias currents only.

The typical dependence of the reduced voltage modulation on the bias current  $I$  at different critical currents is shown in (Fig. 2). The curves, corresponding to the different  $I_c$ 's, are shifted along the current axes and for given  $I_c$  each dependence  $V_R(I)$  has a well defined maximum  $V_R(I_{MAX}) = V_{RMAX}$  at the corresponding value of the bias current.

From the equation (11) for a set of fixed values of  $I_c$  we have computed a set of the values of maximum voltage modulation  $V_{RMAX}$  with the corresponding values of bias current  $I_{MAX}$ . In this way we have obtained the table of values  $V_{RMAX}(I_c; I_{MAX})$ . With the aid of the table we draw the dependence  $V_{RMAX}(I_c)$ , which is shown



in Fig. 3. It is obvious, that this curve gives the upper bound of  $V$  for any symmetric DC SQUID. The different points on the curve correspond to the different bias currents  $I_{M \text{ AX}}$ , at which  $V$  reaches its maximum.

However, as was mentioned above, the critical current of high- $T_C$  interferometer cannot be measured directly with a good accuracy because of large thermal fluctuations. Therefore, it is useful in practice to use the dependence of the maximum modulation signal  $V_{M \text{ AX}}$  on the corresponding value of the bias current  $I_{M \text{ AX}}$ . Such dependence, obtained from the table of values  $V_{R \text{ M AX}}(I_C; I_{M \text{ AX}})$ , is shown on Fig. 4. The different points on this curve belong to the different values of  $I_C$ . Every point on the curve is the maximum point on the corresponding curve from Fig. 2.

The characteristic feature of these two curves  $V_{R \text{ M AX}}(I_C)$  and  $V_{R \text{ M AX}}(I_{M \text{ AX}})$  is the saturation of  $V_{R \text{ M AX}}$  at large critical ( $I_C > 50 \text{ A}$ ) and bias currents. From the curve shown on Fig. 3 the critical current can be obtained from the measured value of  $V_{M \text{ AX}}$ . In addition, this dependence allows one to predict the maximum voltage modulation  $V_{M \text{ AX}}$ , if the critical current of a SQUID is known from the direct measurements.

The influence of inductance on  $V_{M \text{ AX}}$  at different values of the noise parameter, is shown on Fig. 5. The curves were calculated from Eq. (11). It can be seen, that the increase of SQUID inductance leads to the reduction of the voltage modulation in accordance with the scaling law  $\exp(-L/2L_F)$ . In addition, the increase of the noise parameter, also leads to the decrease of the voltage modulation.

## B. Critical current

As is known, it is difficult to measure the critical current of high- $T_C$  Josephson junctions with a good accuracy because VCC is washed out by the thermal fluctuations. This problem can be solved, if we relate the critical current with bias current  $I_{M \text{ AX}}$ , which can be measured directly in SQUID scheme. The idea was realized in the paper<sup>14</sup>, where, based on the numerical simulations of the paper<sup>16</sup>, the following approximate expression for  $I_{M \text{ AX}}$  has been suggested:

$$I_{M \text{ AX}} = 2I_C \left( 1 + \frac{P}{2} \right) \quad (25)$$

From Eq. (25) the critical current can be expressed in terms of the well measured bias current,  $I_{M \text{ AX}}$ :

$$I_C = \frac{I_{M \text{ AX}}}{2} + \frac{k_B T}{0} \left( 1 + \frac{r}{1 + \frac{I_{M \text{ AX}}}{k_B T}} \right) \quad (26)$$

which for  $T = 77\text{K}$  becomes:

$$I_C = \frac{I_{M \text{ AX}}}{2} + 0.514 \left( 1 + \frac{P}{1 + 1.945 I_{M \text{ AX}}} \right) \quad (27)$$

where  $I_C, I_{M \text{ AX}}$  are in  $\text{A}$ .

The Eq. (25) has been obtained for low- $T_C$  junctions<sup>16</sup> and applied to high  $T_C$  SQUIDs in<sup>14</sup>. Therefore, it is interesting to compare (26) with our theory. As is seen from Fig. 2, the expression (11) establishes a single-valued dependence between the critical current and the bias current. The bias current is the well-measured parameter in SQUID scheme. If  $I_{M \text{ AX}}$  is known from the experiment the expression (11) permits to find the critical current at which the voltage modulation reaches its maximum. From (11) for a set of critical current values,  $I_C$  we have found a set of the bias currents  $I_{M \text{ AX}}$ , which give the maximum voltage modulation. The comparison of D rung's expression (27) with our theory is shown on Fig. 6. As is seen from the figure D rung's expression (27) (solid line) and the theory (crosses) give approximately similar results. The deviation between D rung's curve and theoretical points is no more than 10% in the whole range of  $I_{M \text{ AX}}$ 's.

Below we compare the analytical expression (11) with the results of the computer simulations of the stochastic DC SQUID equations (1) and (2), obtained by other authors. The normalized voltage modulation  $V/R I_C$  as a function of the bias current at the different SQUID inductances is shown on Fig. 7. The curves marked by black stars are the theoretical ones, calculated from Eq. (11) (the curves for  $L = 94\text{pT}$ ,  $L = 157\text{pT}$ ) and from the Ambegaokar-Halperin expressions (7), (8) (the curve for  $L = 0$ ). The curves marked by open circles obtained by computer simulations of exact stochastic equations (1) and (2)<sup>17</sup>. All calculations and simulations were made for  $T = 77\text{K}$  and noise parameter  $\beta = 1$  ( $I_C = 3.23 \text{ A}$ ). As is seen from Fig. 7, the simulated curves are close to the calculated ones. Therefore, our expression (11) is a good approximation of the exact solution of stochastic equations (1) and (2).

In addition, we compare our theory with the two well known expressions for the maximum transfer function,  $V = dV/dI$  which have been obtained by the empirical fit to the computed values obtained from the simulations of



the exact stochastic equations of DC SQUID. The first expression is obtained in [6] and is valid for  $\beta = 0.5$ ,  $\beta = 1$ :

$$\frac{V_{MAX}}{I_C R} = \frac{h}{(1 + \beta) (80 \beta^{0.4} + 0.35 (4 \beta)^{2.5})} \quad (28)$$

The second one is the widely used expression of Enpuku<sup>4</sup>:

$$\frac{V_{MAX}}{I_C R} = \frac{4}{(1 + \beta)} \exp \left( -3.5 \frac{k_B T L}{\Phi_0} \right) \quad (29)$$

Here the transfer function was recalculated to  $V$  ( $V = V_0 = 0$ ) assuming a sine shape of the voltage-to- $\Phi$  curve. The comparison of our theory with expressions (28) and (29) for several values of the inductances is shown on Fig. (8).

It is seen, that the theoretical curve (11) and the curve of Enpuku (29) reach the saturation at approximately  $I_C > 40$  A while the curve of Kleiner (28) has a constant non vanishing slope. This slope is probably due to the fact that the right hand side of (28) is equal, in fact, to the transfer function  $V$  which has actually been calculated in [6]. For relatively high critical currents (small  $\beta$ 's) the sine approximation ( $V = V_0 = 0$ ) we made for the shape of the signal is not very good due to the distortion of the signal shape. It is also worth noting that the SQUID inductance affects  $V_{MAX}$  in different ways. The Eq. (28) always gives the highest values, except for  $\beta = 2$  for  $I_C < 80$  A (Fig. 8d). The Eq. (29) always gives the lowest values, except for  $\beta = 1$  (Fig. 8a). For large inductances  $\beta > 2$  the theoretical curve is always higher. The influence of inductance is more pronounced for the voltage modulation given by Eqs. (28) and (29). For example, for  $I_C = 100$  A from  $\beta = 1$  to  $\beta = 2.5$  the theoretical voltage modulation is reduced by a factor of two, while the reduction factor for the Kleiner's and Enpuku's expressions is six and nine, respectively.

#### C. Asymmetric DC SQUID

The numerical simulations of stochastic differential equations, which govern the dynamics of DC SQUID are very time consuming for practical high  $T_C$  DC SQUIDs due to the large thermal fluctuations and large loop inductance. This is why in most cases the investigations of asymmetric DC SQUID are restricted to the computer simulations in small inductance limit ( $\beta \ll 1$ )<sup>10,11,12,13,14</sup>. Since our theory is valid for asymmetric SQUIDs with large inductance we cannot compare it with the results of other authors obtained for asymmetric SQUIDs with small inductance.

The practical importance of asymmetric DC SQUIDs is that they have a higher transfer function (the slope of the voltage-to- $\Phi$  curve) as compared to the symmetric case<sup>10,11,12,13,14</sup>. This property is generally attributed to the distortion of the voltage-to- $\Phi$  curve. The shape of this curve significantly differs from the sine shape that results in the high steep of the slope. For large inductance SQUID the voltage-to- $\Phi$  curve has a sine shape as evident from Eq. (16). Therefore, we carefully studied the influence of the junction asymmetry of large inductance interferometers on the voltage modulation. We have found that in the large range of asymmetry parameters the voltage modulation of asymmetric DC SQUID with large inductance can be significantly higher than that for symmetric SQUIDs.

In principle, the asymmetry parameters  $\alpha$  and  $\beta$  are independent of each other and, therefore, they may present in the junctions in any combination. From our calculations we have chosen for presentation here only three types of the junction asymmetry which generally give a correct picture of how the voltage modulation is influenced by any type of asymmetry. Below we present the numerical results for the current asymmetry ( $\alpha = 0$ ;  $\beta \neq 0$ ), the resistance asymmetry ( $\alpha \neq 0$ ;  $\beta = 0$ ) and the geometric asymmetry ( $\alpha = \beta \neq 0$ )<sup>1</sup>. The effect of different types of the junction asymmetry on the dependence of the voltage modulation on the critical current is shown on Fig. 9 and Fig. 10. As is seen from the figures, the general trends of the asymmetry are the increase of the voltage modulation and non vanishing slope of the curves as compared with the symmetric junctions. The slope being increased with the increase of the asymmetry. For the geometric asymmetry the increase of the voltage modulation is seen in the whole range of the critical currents (Fig. 9), while for the current or resistance asymmetry there exists the range of relatively small critical currents (approximately less than 10 A) where the voltage modulation of asymmetric DC SQUID is lower than that of the symmetric one (Fig. 10). In order to clarify the picture we made a careful study of the dependence of  $V_{RMAX}$  on the asymmetry parameters at the given values of the critical current. It appears there exists some threshold value of the critical current, approximately in the vicinity of 8 A, which divides the whole range of the critical currents in two parts. Below the threshold the current and resistance asymmetry always leads to the decrease of the voltage modulation as compared to symmetric DC SQUID (Fig. 11a, Fig. 11b). The geometric asymmetry does not change the voltage modulation up till approximately  $\beta = 0.5$  with the subsequent decrease of the voltage modulation (Fig. 11c). Above the threshold the curves  $V_{RMAX}$  ( $\alpha = 0$ ;  $I_C = \text{const}$ ) and  $V_{RMAX}$  ( $\alpha = 0$ ;  $I_C = \text{const}$ ) have a clear maximum approximately at the vicinity  $\beta = 0.25$  and  $\beta = 0.25$ , respectively (Fig. 12a, Fig. 12b). This



maximum lies approximately 1.5 times higher a symmetric value for the voltage modulation for current asymmetry and 1.3 times higher a symmetric value for the voltage modulation for resistance asymmetry. It is worth noting that in the wide range of the current asymmetry ( $0 < \alpha < 0.7$ ) or of the resistance asymmetry ( $0 < \beta < 0.7$ ) the voltage modulation is higher than its symmetric value. However, the geometric asymmetry leads to the significant increase of the voltage modulation in the whole range of the critical currents (Fig. 12c).

#### IV . COMPARISON WITH EXPERIMENT

In order to compare our theory with experiment we took two groups of DC SQUIDS. The first group comprised about 50 SQUIDS which have been chosen before for the same purpose<sup>18, 19</sup>. All of these SQUIDS are single layer ones, using 100 or 200 nm thick  $\text{YBa}_2\text{Cu}_3\text{O}_{7-x}$  films deposited by laser ablation onto  $\text{SrTiO}_3$  bicrystal substrates with 24 or 30 m isorientation angles, both having symmetrical configuration. The technology is described in detail in<sup>20</sup>. The second group comprised 10 bicrystal SQUIDS, which were also single layer ones, using 150–200 nm thick  $\text{YBa}_2\text{Cu}_3\text{O}_{7-x}$  films deposited by linear hollow cathode sputtering onto  $\text{SrTiO}_3$  bicrystal symmetrical substrates with 24 m isorientation angle<sup>21</sup>. All SQUIDS have  $\phi = 1$  and  $\beta = 0.05$  and all measurements were performed in liquid nitrogen at 77 K.

Since the critical current,  $I_c$  of a high  $T_c$  DC SQUID cannot be measured with a good accuracy due to high level of thermal fluctuations, we here, for the comparison with experiment, use only the quantities, which are measured directly,  $V_{MAX}$  and  $I_{MAX}$ . The dependence  $V_{R,MAX}(I_{MAX})$  for symmetric SQUID together with experimental points is shown on Fig. 13. It can be seen, that there is a significant deviation of experimental points from theoretical line of symmetric DC SQUIDS. Part of the experimental points which lie above theoretical line can be explained by the junction asymmetry. In order to show this we add to the plot of Fig. 13 the theoretical curves for asymmetric DC SQUID (Fig. 14a and Fig. 14b). We choose a significant asymmetry on these graphs ( $\alpha = 0.9$ ;  $\beta = 0.9$ ) in order to mark the borders of the possible scattering of the voltage modulation values. In addition, the asymmetry allows one to explain the experimental points which lie below the symmetric line at small bias currents  $I_{MAX} < 10$  A. Since at small bias currents  $I_{MAX}$  is close to  $I_c$  (see Eq. (27)) this reduction of the voltage modulation is consistent with the result of section IIIC where we showed that at relatively small critical currents a junction asymmetry reduced the voltage modulation. Therefore, the junction asymmetry can explain the experimental values of the voltage modulation which lie above the line for symmetric DC SQUID and the points which lie below symmetric line at small bias currents. However, a significant reduction of the voltage modulation, which lies well below a symmetric line in Figs. 13 and 14 cannot be explained by the junction asymmetry. A possible explanation of these points is the presence of relatively large amplitude of a second harmonic in the junction current phase relation<sup>19</sup>.

#### V . CONCLUSION

In the paper we consistently compared the analytical theory for the voltage-current characteristics of the large inductance ( $L > 100\text{pH}$ ) high- $T_c$  DC SQUIDS that has been developed previously<sup>7,8</sup> with the computer simulations and the experiment. It is shown that the theoretical voltage modulation for symmetric junctions is in a good agreement with the results of known computer simulations. It is also shown that the asymmetry of the junctions results in the increase of the voltage modulation in the large range of critical currents and asymmetry parameters. We compared our theory with the experimental values of the voltage modulation. It appeared that the asymmetry can explain a large portion of experimental values of the voltage modulation which lie above the theoretical curve for symmetric DC SQUID. It also explains experimental points which lie below the curve at small critical currents. However, a significant portion of these values which lie below the curve cannot be explained by the junction asymmetry. From our opinion a possible explanation of these low lying points is the presence of relatively large amplitude of a second harmonic in the junction current phase relation<sup>19</sup>.

#### Acknowledgments

We thank R. Kleiner for providing us with the unpublished results of the numerical simulations shown in Fig. 7 of the paper. We are also grateful to V. Schultze and R. Kleiner for fruitful discussion.



The authors acknowledge the support by the INTAS grant 2001-0809.

- 
- <sup>1</sup> J. Beyer, D. D rung, F. Ludwig, T. M inotani, K. Enpuku, Appl. Phys. Lett. 72, 203 (1998) .
  - <sup>2</sup> K. Park, S.-G. Lee, H. C. Kwon, Y. K. Park, J.-C. Park, IEEE Trans. Appl. Supercond. 5, 3119 (1995) .
  - <sup>3</sup> Q. Jia, F. Yan, C. M ombourquette, D. Reagor, Appl. Phys. Lett. 72, 3068 (1998).
  - <sup>4</sup> K. Enpuku, G. Tokita, T. Manuo, and T. M inotani, J. Appl. Phys. 78, 3498 (1995) .
  - <sup>5</sup> B. Chesca, J. Low Temp. Phys. 112, 165 (1998).
  - <sup>6</sup> D. K oelle, R. K leiner, F. Ludwig, E. D ankster, John C larke, Rev. Mod. Phys. 71, 631 (1999).
  - <sup>7</sup> Ya. S. G reenberg, Physica C 371, 156 (2002).
  - <sup>8</sup> Ya. S. G reenberg, Physica C 383, 354 (2003).
  - <sup>9</sup> V. Ambegaokar and B. I. Halperin, Phys. Rev. Lett. 22, 1364 (1969).
  - <sup>10</sup> G. Testa, S. Pagano, M. Russo, E. Samelli, EUCAS'99, Inst. Phys. Conf. Ser. 167, 529 (1999).
  - <sup>11</sup> M uller J., S. W eiss, R. G ross, R. K leiner, D. K oelle, IEEE Trans. Appl. Supercond. 11, 912 (2001).
  - <sup>12</sup> K. Enpuku, T. M itonani, A. K andori, F. Shiraishi, J. Beyer, D. D rung, F. Ludwig, Jpn. J. Appl. Phys. Pt. 1, 37, 4769 (1998).
  - <sup>13</sup> G. Testa, C. G ranata, C. C alidonna, C. D i Russo, M. M angio Fumari, S. Pagano, M. Russo, E. Samelli, Physica C 368, 232 (2002).
  - <sup>14</sup> D. D rung, F. Ludwig, W. M uller, U. Steinho , L. Trahm s, Y. Q. Shen, M. B. Jensen, P. Vase, T. Holst, T. Freltoft, Appl. Phys. Lett. 68, 1421 (1996).
  - <sup>15</sup> V. A. K hlus, I. O. Kulik, Zhurnal Techn. Fiziki 45, 449 (1975) (in Russian).
  - <sup>16</sup> R. F. Voss J. Low Temp. Phys. 42, 151 (1981).
  - <sup>17</sup> R. K leiner, private communication.
  - <sup>18</sup> Ya. S. G reenberg, V. Schultze, H.-G. M eyer, Physica C 368, 236 (2002).
  - <sup>19</sup> I. Ya. S. G reenberg, I. L. Novikov, V. Schultze, H.-G. M eyer, Eur. J. Phys. B 44, 57 (2005).
  - <sup>20</sup> R. IJsselsteijn, H. Elsner, W. M orgenroth, V. Schultze, and H. G. M eyer, IEEE Trans. on Appl. Supercond. 9, 3933 (1999).
  - <sup>21</sup> M. Lindstroem , A Thesis of Master degree, Espoo March 9 (1999).



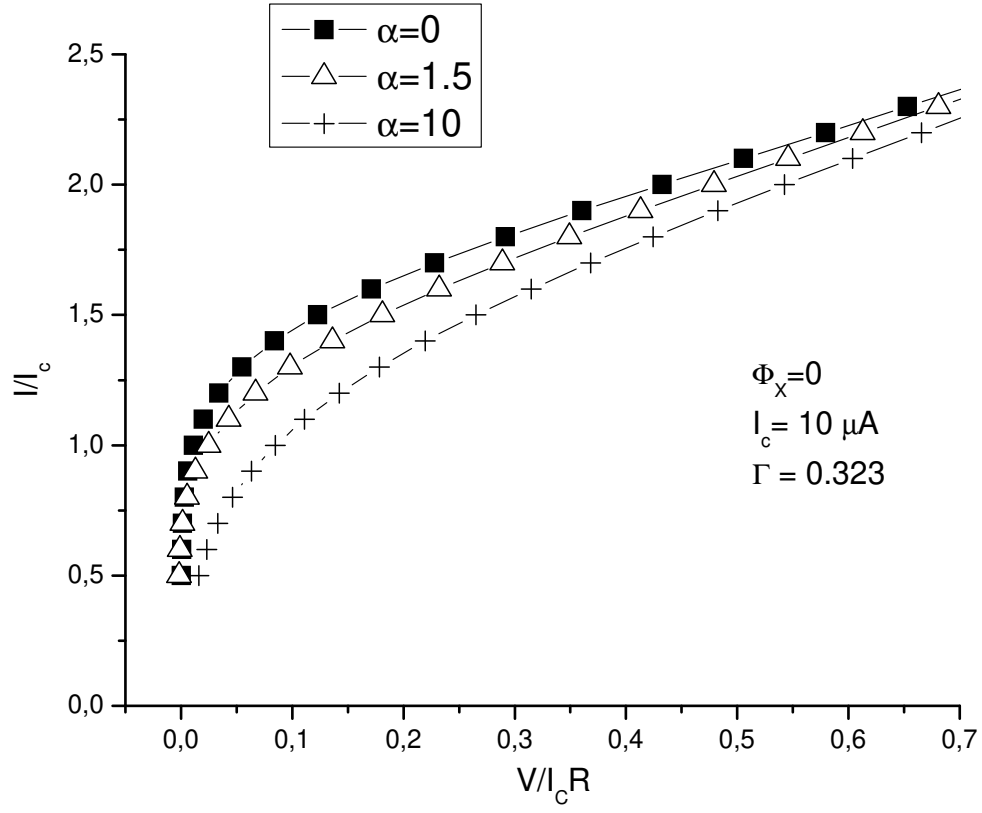


FIG. 1: VCC of symmetric DC SQUID at zero magnetic field and different inductances.  $I_c = 10 \text{ A}$ ,  $T = 77\text{K}$ , the curve with  $\alpha = 0$  (black box) was calculated from expression (7), the curves with  $\alpha = 1.5$  (triangle) and  $\alpha = 10$  (cross) were calculated from the expression (10).



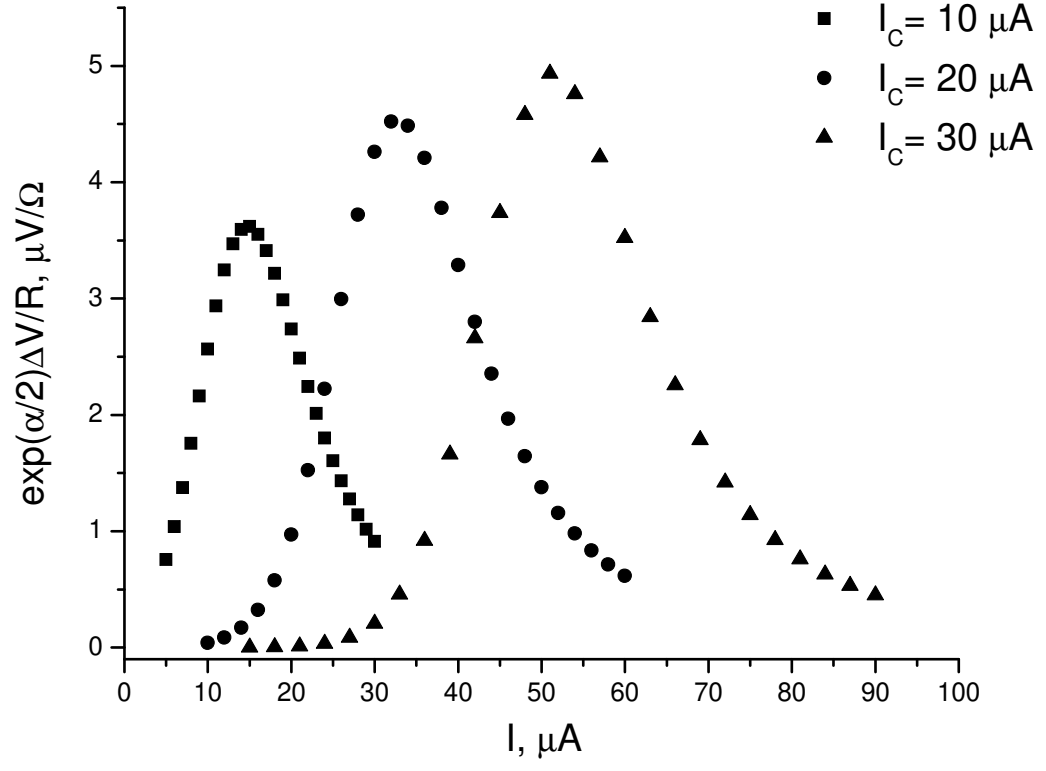


FIG. 2: The reduced voltage modulation vs bias current curves at different values of the critical current for symmetric DC SQUID.



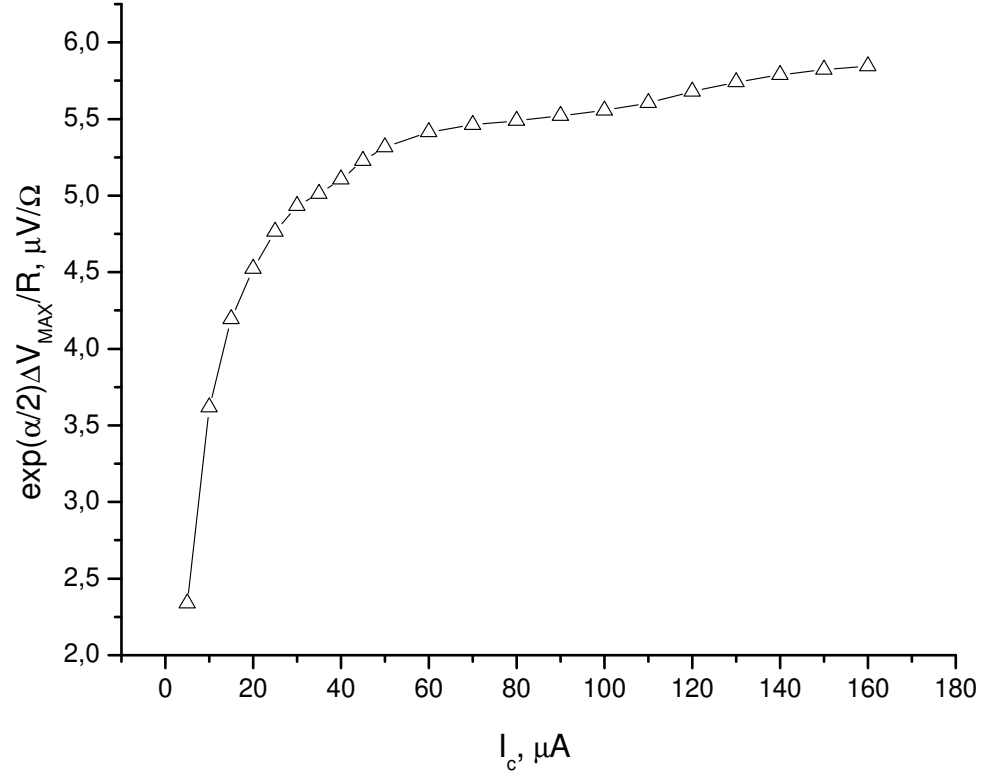


FIG. 3: The maximum value of the reduced voltage modulation,  $V_{R,MAX}$  vs critical current. The different points on the curve correspond to the different bias currents  $I_{MAX}$ , at which  $V$  reaches its maximum.



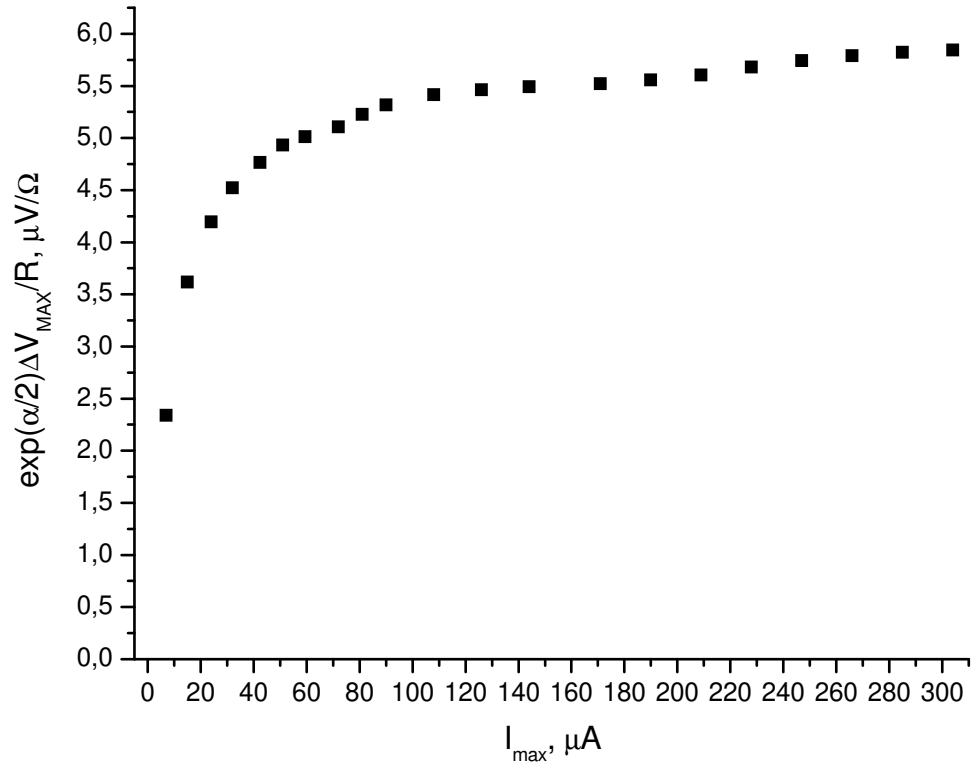


FIG . 4: Dependence of the maximum value of the reduced voltage modulation  $V_{R, \text{MAX}}$  on the bias current  $I_{\text{MAX}}$ .



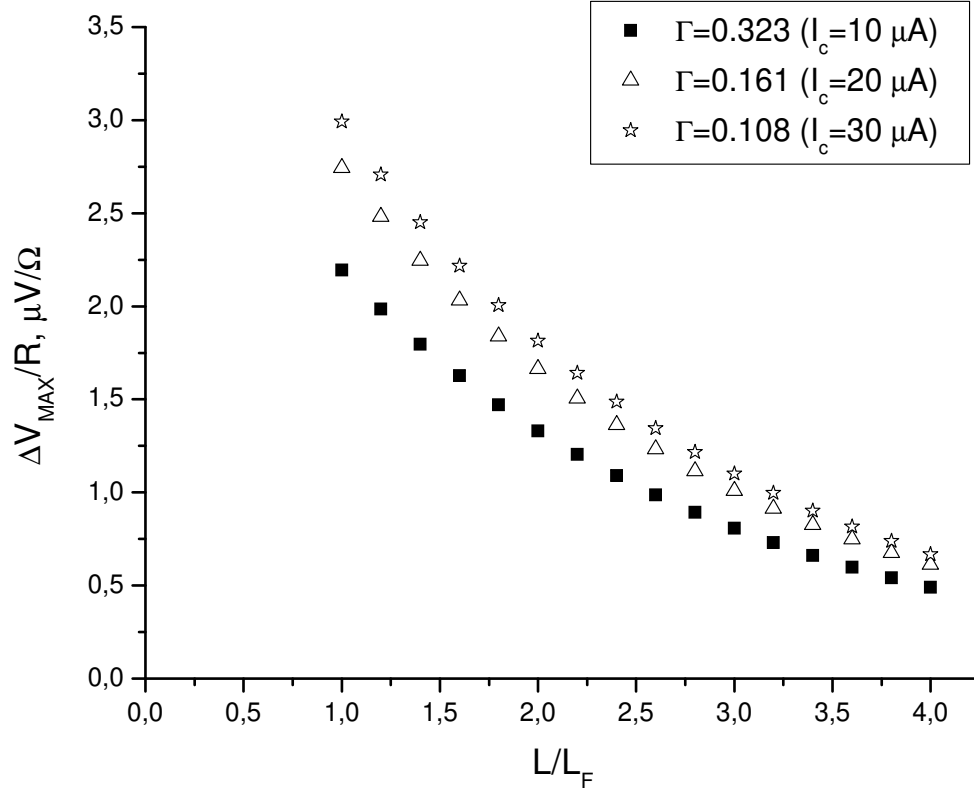


FIG . 5: The dependence of the maximum value of the voltage modulation  $\Delta V_{MAX}/R$  on the inductance for symmetric DC SQUID ; (black box)-  $\Gamma = 0.323$  ( $I_c = 10 \mu A$ ) ; (triangle)-  $\Gamma = 0.161$  ( $I_c = 20 \mu A$ ) ; (star)-  $\Gamma = 0.108$  ( $I_c = 30 \mu A$ ) .



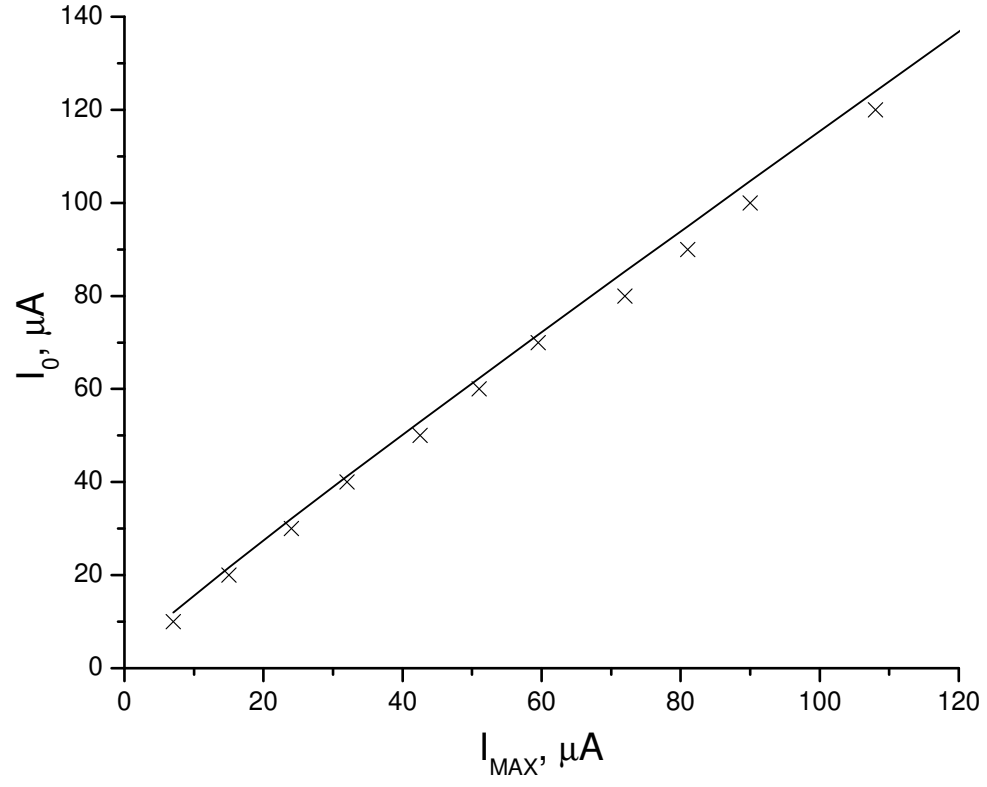


FIG . 6: The dependence of the SQUID critical current  $I_0 = 2I_C$  on the bias current  $I_{MAX}$ . Solid line is the expression of Drung (Eq. (27)); crosses are theoretical points obtained from Eq. (11).



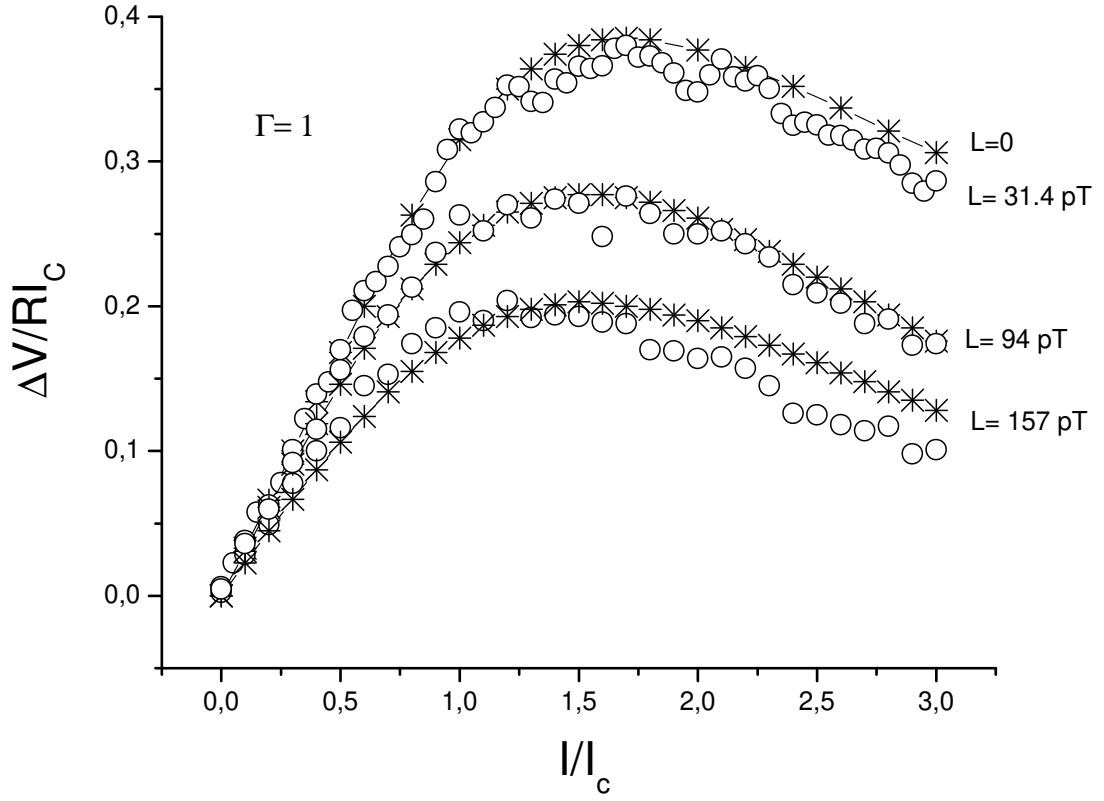


FIG. 7: The dependence of the normalized voltage modulation on the bias current. Comparison of theory (stars) with the simulation of Kleiner (open circles). The curve for  $L = 0$  was calculated from (7) and (8), the curves for  $L = 94 \text{ pT}$ ,  $L = 157 \text{ pT}$  were calculated from (11). All calculations are made at  $77 \text{ K}$  for  $\Gamma = 1$ .



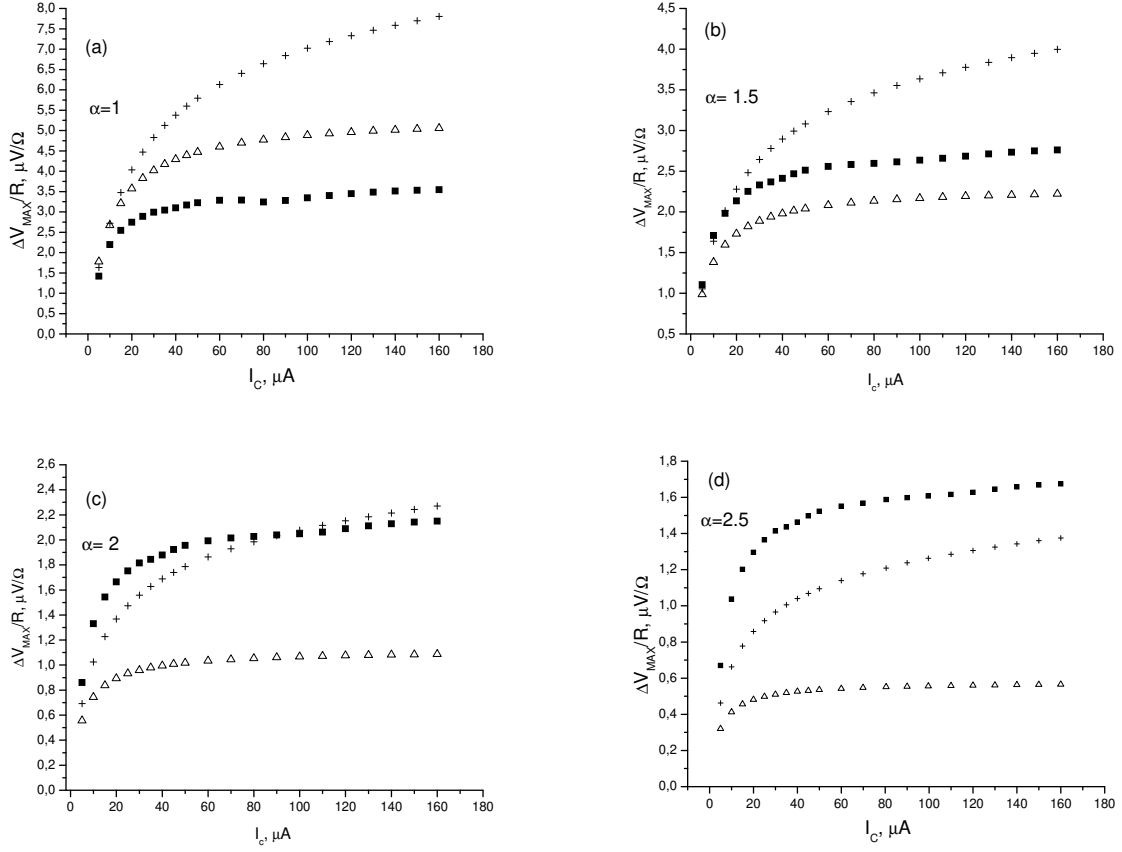


FIG. 8: The comparison of the maximum voltage modulation given by (Eq. (11)), (black box) with those obtained from the expressions of Kleiner (Eq. (28)), (cross) and Enpuku (Eq. (29)), (triangle) for: (a)  $\alpha = 1$ ; (b)  $\alpha = 1.5$ ; (c)  $\alpha = 2$ ; (d)  $\alpha = 2.5$ .



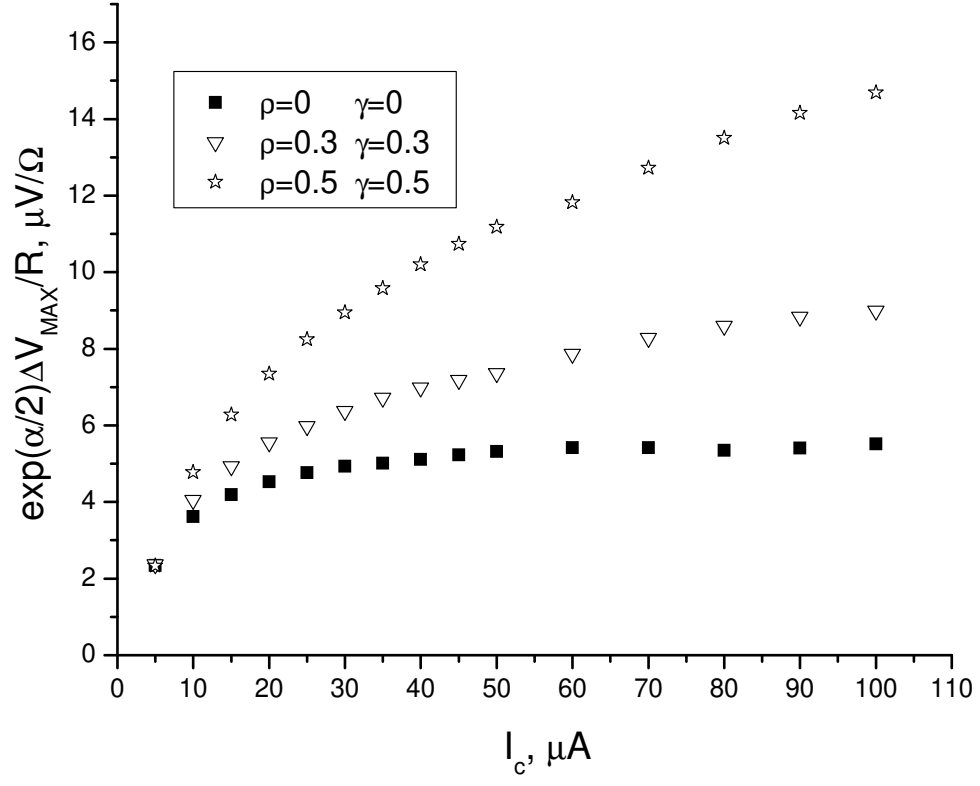


FIG . 9: The influence of the geometric asymmetry on the maximum voltage modulation,  $V_{R \text{ MAX}}$ .



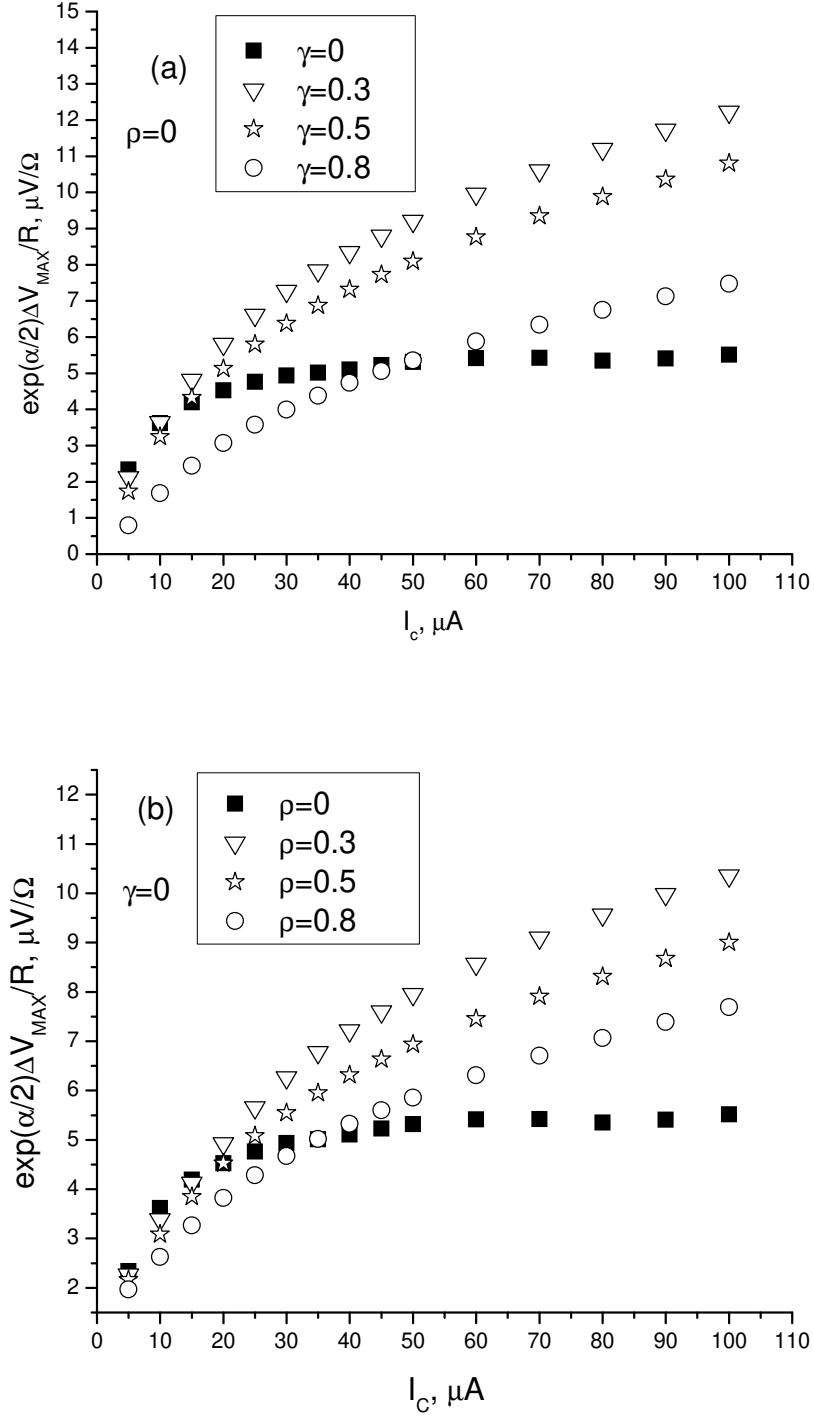


FIG. 10: The dependence of the maximum voltage modulation,  $V_{R, \text{MAX}}$  on the critical current for two types of asymmetry: a) the current asymmetry ( $\rho = 0$ ); b) the resistance asymmetry ( $\gamma = 0$ )



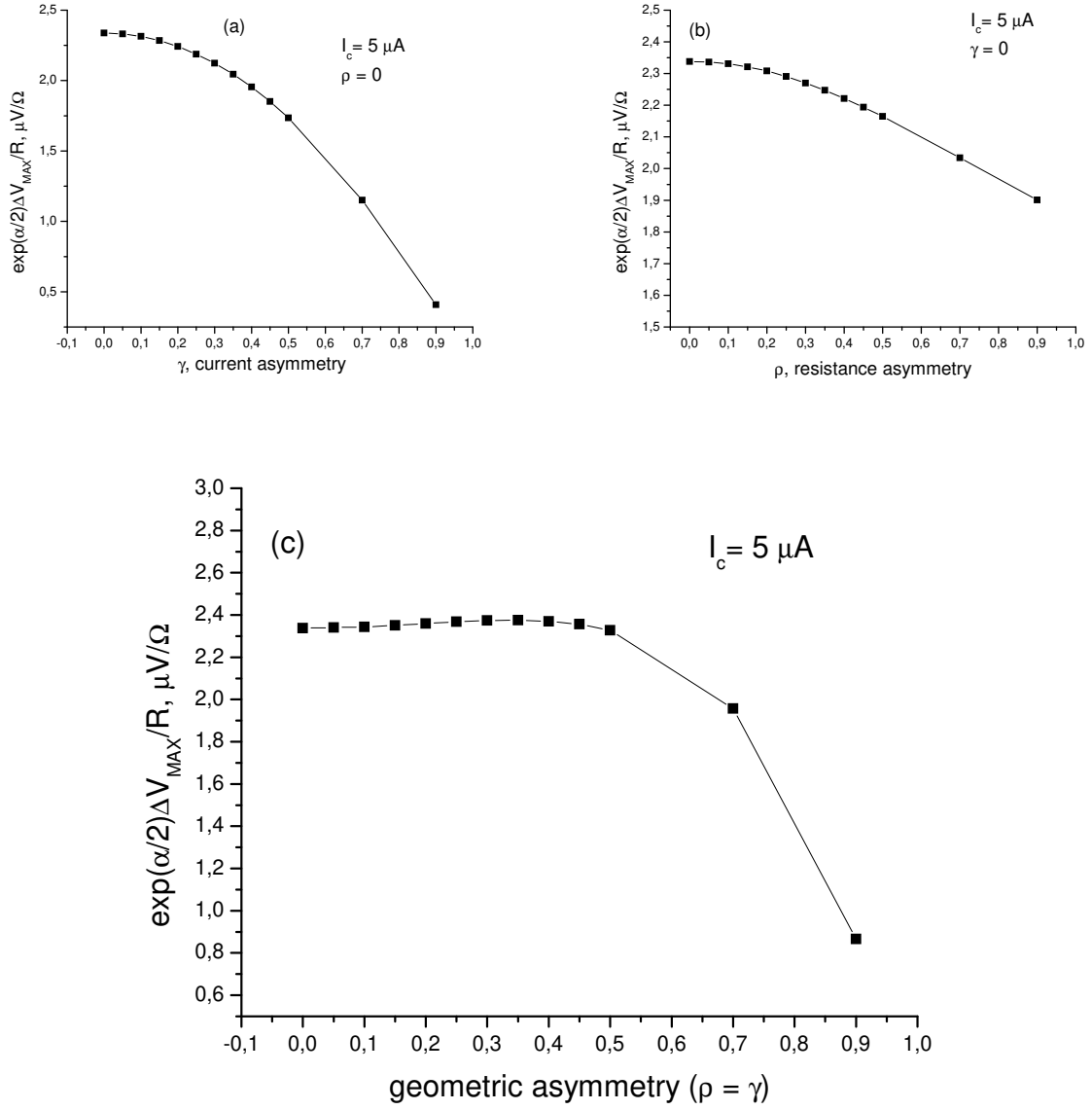


FIG. 11: The dependence of reduced maximum voltage modulation on the asymmetry parameters at  $I_c = 5 \text{ A}$  for three types of asymmetry: a)  $\rho = 0$ ;  $\gamma \neq 0$ ; b)  $\gamma = 0$ ;  $\rho \neq 0$ ; c)  $\rho = \gamma \neq 0$ .



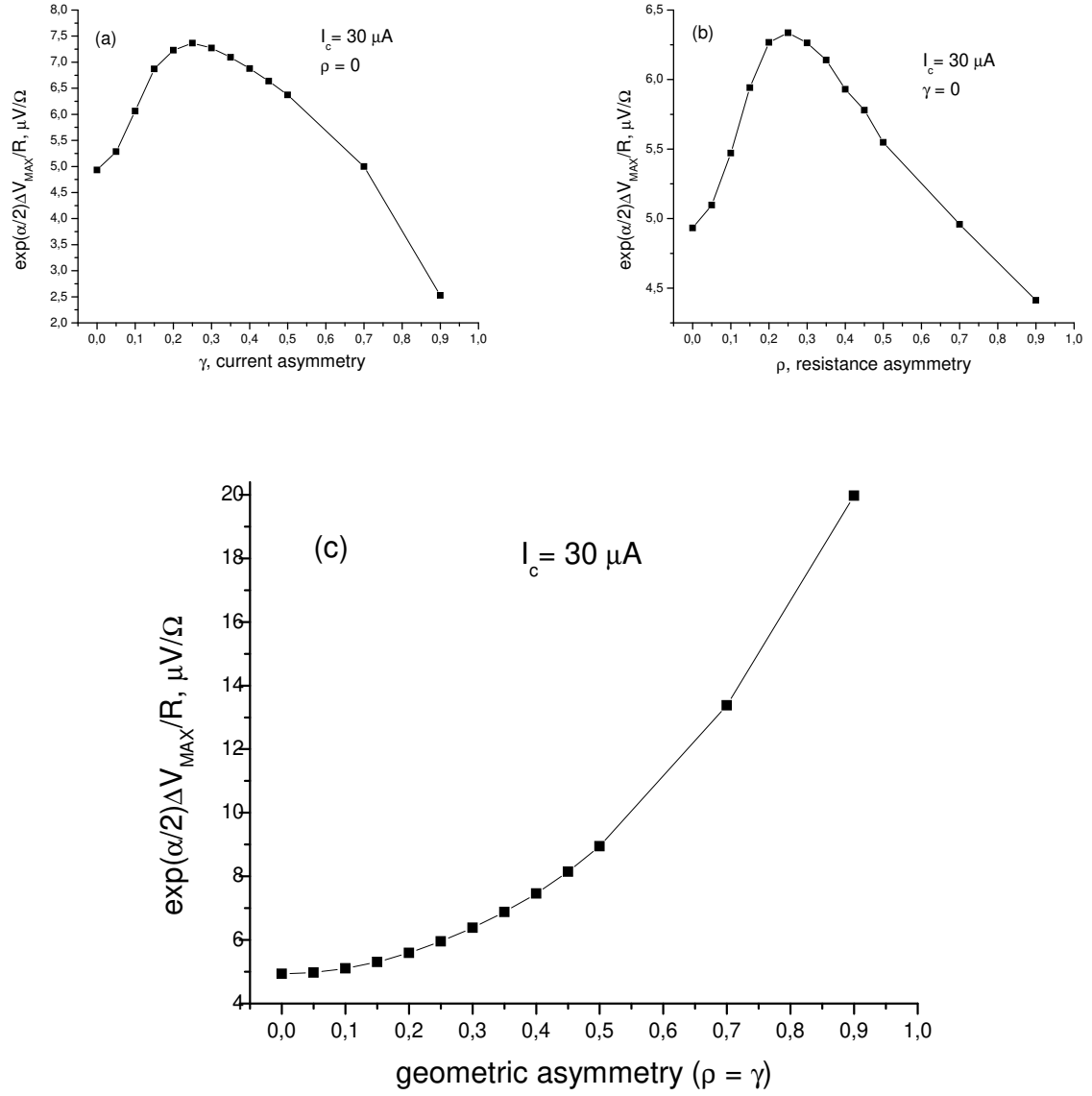


FIG. 12: The dependence of reduced maximum voltage modulation on the asymmetry parameters at  $I_c = 30 \text{ A}$  for three types of asymmetry: a)  $\rho = 0$ ;  $\gamma \neq 0$ ; b)  $\gamma = 0$ ;  $\rho \neq 0$ ; c)  $\rho = \gamma \neq 0$ .



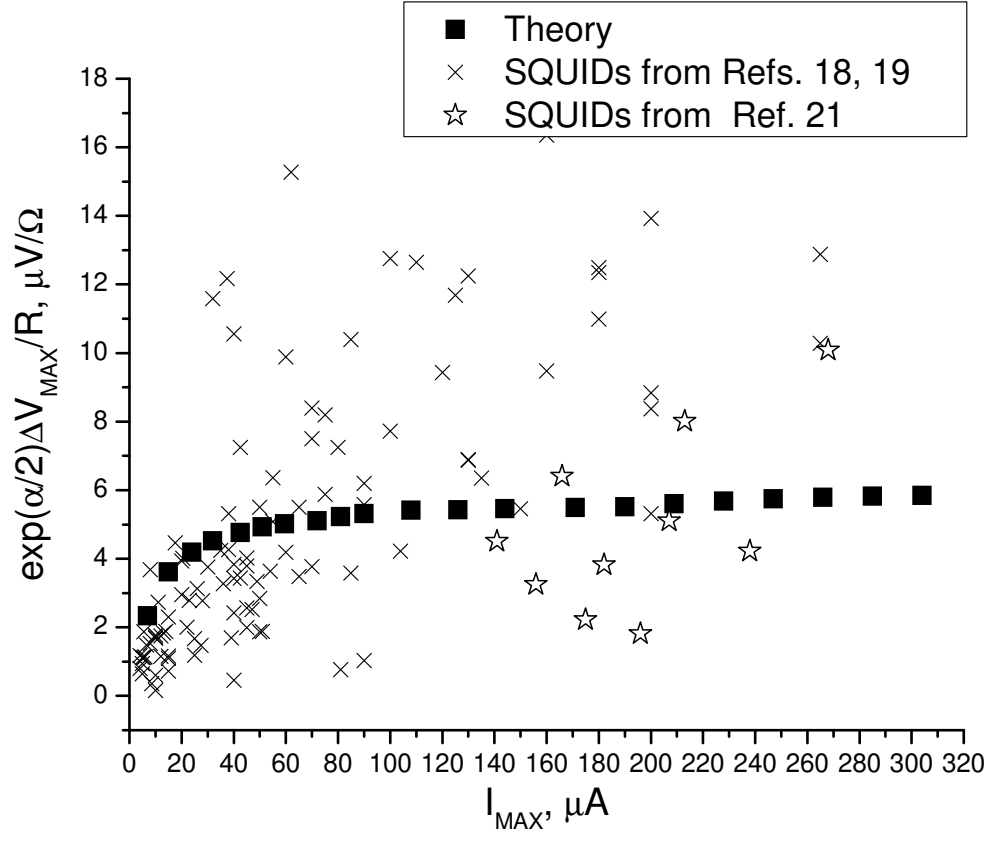


FIG. 13: The dependence  $V_{R, \text{MAX}}(I_{\text{MAX}})$  for symmetric SQUID together with experimental points.



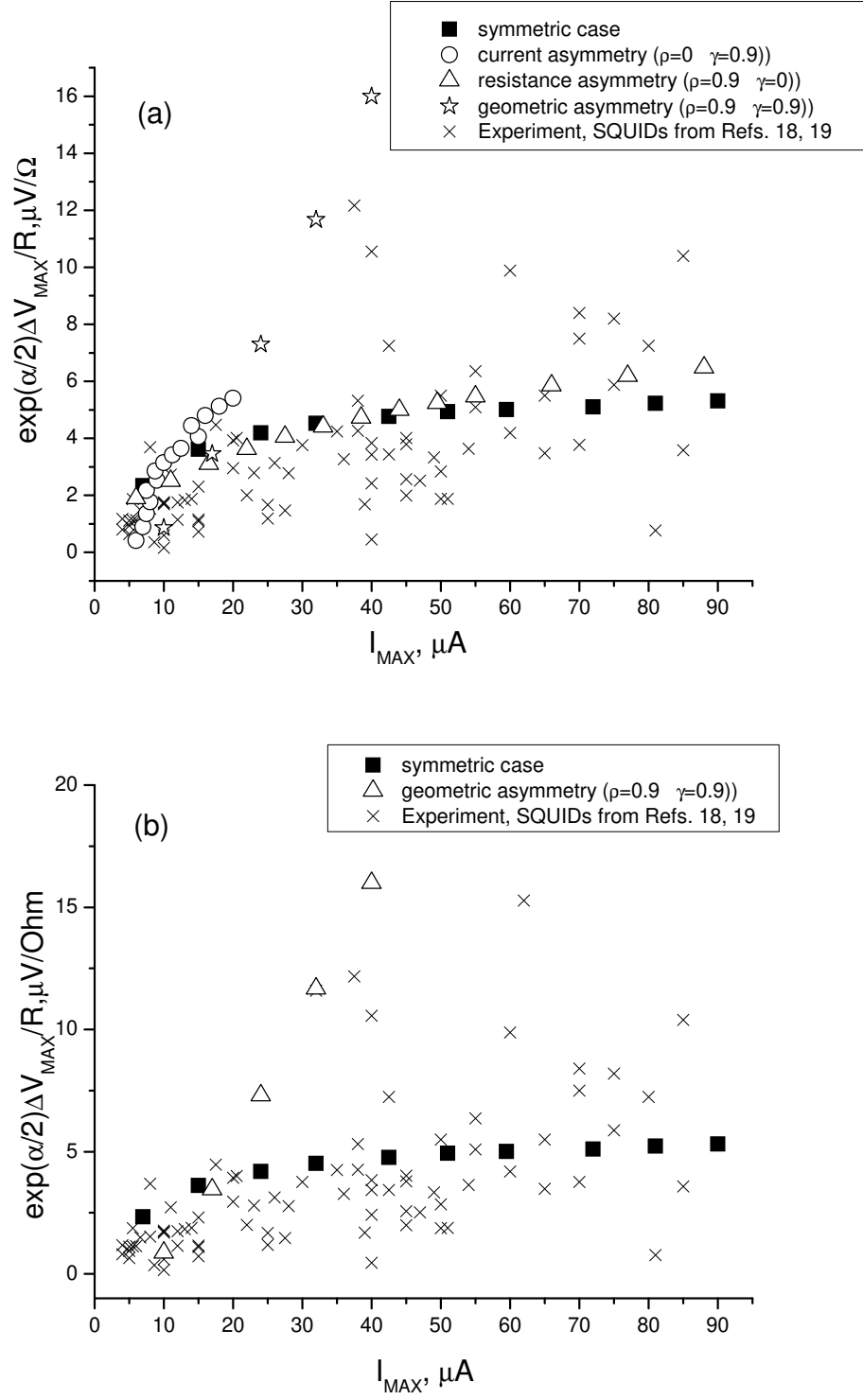


FIG. 14: The dependence  $\Delta V_{\text{MAX}}(I_{\text{MAX}})$  for symmetric and asymmetric SQUIDs together with experimental points.